Experimental Study of Zeeman Light Shifts in Weak Magnetic Fields

Claude Cohen-Tannoudji and Jacques Dupont-Roc
Laboratoire de Spectroscopie Hertzienne de l'Ecole Normale Superieure, Associe au Centre National de la Recherche Scientifique, Paris, France
(Received 19 May 1971)

According to the quantum theory of the optical-pumping cycle, one can describe the effect of a nonresonant light beam on the different Zeeman sublevels of an atomic ground state by an effective Hamiltonian $\mathcal{H}_e$ which depends on the polarization and spectral profile of the incident light. In order to check the structure of $\mathcal{H}_e$, we have performed a detailed experimental study of the ground-state energy sublevels of various kinds of atoms perturbed by different types of nonresonant light beams. Attention is paid to the modification of the Zeeman structure due to $\mathcal{H}_e$. We have been able to obtain experimentally in the ground state of ^{199}Hg, ^{201}Hg, and ^{87}Rb, Zeeman light shifts that are larger than the width of the levels due to the thermal relaxation. The removal of the Zeeman degeneracy in zero external field, due to a nonresonant light irradiation, is observed by different optical-pumping techniques; the full Zeeman diagram of the perturbed atoms is also determined when a static field $\vec{H}_0$ is added. We have checked that the effect of $\mathcal{H}_e$ can be described in terms of fictitious static electric or magnetic fields. These fictitious fields can be used to act selectively on a given atomic level.

INTRODUCTION

The ground state of a two-level atom is broadened and shifted when irradiated by a light beam. The lifetime T'_P is due to the resonant photons of the light wave (the atom can actually leave the ground state by absorption of such a photon). The energy shift $\Delta E'$ can be described in terms of virtual absorptions and reemissions of the nonresonant photons, which mix the excited- and ground-state wave functions.[1] It may be also interpreted as a dynamic Stark effect in the electric field of the light wave.[2,3] If the ground state has a nonzero angular momentum F, the effect of a nonresonant irradiation ($\Delta E' \gg 1/T'_P$) on the $2F+1$ sublevels is described by an effective Hamiltonian $\mathcal{H}_e$. The energy levels of the perturbed atom are the eigenstates of $\mathcal{H}_e$. $\mathcal{H}_e$ is a function of the intensity, of the polarization, and of the spectral profile of the light.

In this paper, we report the results of an *experimental* study of the ground-state energy sublevels of various kinds of atoms perturbed by different types of nonresonant (nr) light beams.

The expression of $\mathcal{H}_e$ has been theoretically established in a quantum theory of the optical pumping cycle.[4] As in various atomic physics problems,[5,6] the use of irreducible tensor operators has greatly simplified the analysis of $\mathcal{H}_e$.[3] We emphasize the fact that the form of $\mathcal{H}_e$ (eigenstates, relative spacing of the energy sublevels) is in many cases determined only by the angular properties of the light beam, especially by its polarization. As pointed out by several authors,[7-9] one can also associate with the light beam fictitious static fields which would produce the same splitting in the ground state and which are very useful to visualize the symmetry properties of $\mathcal{H}_e$.

More precisely, the effect of the light beam is the following. First, it produces a displacement of the ground state as a whole (center-of-mass light shift); second, it removes the Zeeman degeneracy of the level. The first effect has been observed directly on an optical transition by Aleksandrov *et al.*,[10] Bradley *et al.*,[11] and Platz.[12] The difference of the center-of-mass light shifts for two different hyperfine levels of an alkali-atom results in a modification of the hyperfine frequency of the ground state, which has been observed and studied in great detail.[13-15]

Here we focus our attention on the second point, the effect of the light beam inside each ground-state multiplicity, which depends more critically on the symmetries of $\mathcal{H}_e$. With these Zeeman light shifts is associated a shift of the magnetic resonance line, which has been observed by several authors.[16-18] However, these experiments have been performed in a high magnetic field, i.e., when Zeeman splitting is large compared to the light shift. The atomic wave functions are then determined by the Zeeman Hamiltonian and the light beam only modifies slightly the energies. For our purpose, a more interesting situation is the opposite case, when the structure of the ground state is determined mainly by the light beam. For that reason much attention must be paid to the low-field region, including the zero-field case where the eigenstates of $\mathcal{H}_e$ are directly observed. The full Zeeman diagram, deeply modified by the presence of the nr light beam, also gives valuable information on the structure of $\mathcal{H}_e$.

To our knowledge, because of the smallness of the currently obtained light shifts compared to the width of the levels, the energy diagram of an atom sub-

mitted to a nr irradiation has never been experimentally investigated. Using atoms with long relaxation times and powerful discharge lamps, we have observed Zeeman light shifts larger than the width of the levels and we have been able to carry out an experimental study of the energy levels of different kinds of atoms irradiated by nr light beams in zero or nonzero magnetic field. The form of the effective Hamiltonian for various polarizations has been checked in this way and found to be in excellent agreement with the theoretical predictions.

In particular, the concept of the fictitious field appears to be very convenient for interpreting the results of the experiments. Furthermore, we demonstrate that light shifts can practically be used in some experiments to produce static or modulated fictitious fields acting specifically on a given atomic level.

The paper is divided as follows. In Sec. I, the theoretical predictions for $\mathcal{H}_e$ are briefly recalled. In Sec. II, we review the various experimental methods used to study the energy diagram of the perturbed atom. We present in Sec. III the results of experiments performed on ^{199}Hg, ^{201}Hg, and ^{87}Rb atoms. Finally, in Sec. IV some applications of oscillating fictitious fields are investigated.

I. THEORETICAL PREDICTIONS FOR $\mathcal{H}_e$

In this section, we first recall the expression for $\mathcal{H}_e$ and the form of its expansion in irreducible tensor operators (more details may be found in Refs. 3 and 5). We then discuss the consequences of the symmetries of the light beam and show how it is possible to derive in simple cases the coefficients of the expansion of $\mathcal{H}_e$ without any complicated algebra. Finally, we determine the "fictitious" static fields which describe the effect of various types of nr light beams inside the ground-state multiplicities.

A. Effective Hamiltonian $\mathcal{H}_e$

1. *Notations and Assumptions*

(a) The nr light beam B_1 is characterized by its intensity $\mathcal{I}$, its polarization vector $\vec{e}_\lambda$, and its spectral profile $u(k)$ which is centered at the frequency $\bar{k}$ and has a width Δk. We assume Δk much larger than the light shifts and magnetic splittings involved in this study. We take $\hbar = c = 1$.

(b) The interaction of the atom with the light wave is of the electric dipole type. Therefore, the polarization vector $\vec{e}_\lambda$ is the only relevant geometrical parameter of the light beam which has to be considered.

(c) We suppose that B_1 is quasiresonant: $\bar{k}$ is close to a particular absorption frequency of the atom so that we will consider only the corresponding excited state. $|\phi M\rangle$ and $|Fm\rangle$ are, respectively, the hyperfine sublevels of the excited and ground states; $k_{F\phi}$ is the energy difference between those two levels for the free atom in zero field. We assume that in our experiments, the inverse of the excited-state lifetime is always smaller than Δk.

(d) Light shifts and Zeeman splittings in the ground state will be always small compared to the hyperfine structure so that F is a "good quantum number."

2. *Expression of Effective Hamiltonian*

The effect of the light beam inside the F multiplicity[19] is described by the Hamiltonian $\mathcal{H}_e(F)$

$$\mathcal{H}_e(F) = \sum_\phi \mathcal{H}_e(F, \phi) , \tag{1.1}$$

where

$$\mathcal{H}_e(F, \phi) = \Delta E'(F, \phi) A(F, \phi) . \tag{1.2}$$

$\Delta E'(F, \phi)$ is a real number, proportional to the light intensity, and is a function of $\bar{k}$. Its complete expression may be found in Refs. 1 and 4. The shape of its variations with $\bar{k}$ is given in Fig. 1. $\Delta E'(F, \phi)$ is maximum when $\bar{k} - k_{F\phi}$ is of the order of Δk. When $\bar{k}$ is far from $k_{F\phi}$,

$$\Delta E'(F, \phi) \approx (\mathcal{E} d_{F\phi})^2 / (\bar{k} - k_{F\phi}) , \tag{1.3}$$

where $\mathcal{E}$ is the electric field of the light wave, $d_{F\phi}$ the reduced matrix element of the electric dipole operator between the two levels F and ϕ. $\Delta E'(F, \phi)$ changes its sign with $\bar{k} - k_{F\phi}$. $A(F, \phi)$ is an operator depending on the polarization of B_1 and acting inside the F multiplicity:

$$A(F, \phi) = P_F (\vec{e}_\lambda^{\,*} \cdot \vec{D}) P_\phi (\vec{e}_\lambda \cdot \vec{D}) P_F , \tag{1.4}$$

where P_F and P_ϕ are the projection operators onto the F and ϕ multiplicities; $\vec{D}$ is the angular part of the electric dipole operator. $A(F, \phi)$ is obviously Hermitian.

The concept of effective Hamiltonian must be used with some care when several nr beams act simultaneously on the atom. If there is no phase relation between them, $\mathcal{H}_e$ is simply the sum of the effective Hamiltonians associated with each individ-

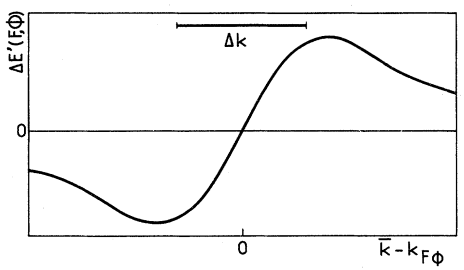

FIG. 1. Variations of $\Delta E'(F, \phi)$ with the mismatch $\bar{k} - k_{F\phi}$ between the mean energy of the incident photons and the energy of the $F \rightarrow \phi$ atomic transition. Δk is the spectral width of the incident light.

ual beam. But if two beams are coherent, time-dependent terms may appear in the effective Hamiltonian.

3. *Expansion of $\mathcal{H}_e$ on an Operator Basis and Introduction of Fictitious Fields*

The basic idea is to develop $\mathcal{H}_e(F)$ on a basis of operators acting inside the ground-state multiplicity. Each term of this expansion may be interpreted as the interaction Hamiltonian of the ground state with a fictitious static field. To illustrate the method, let us first consider the simple case of a level $F = \frac{1}{2}$.

a. A simple case: $F = \frac{1}{2}$. There are only two sublevels in the multiplicity. $\mathcal{H}_e(F)$ is a 2×2 Hermitian matrix which can always be expanded in terms of the unit matrix and the three Pauli matrices $\sigma_i (i = x, y, z)$:

$$\mathcal{H}_e(F) = c_0 + \sum_i c_i \sigma_i \ . \tag{1.5}$$

We interpret $\sum_i c_i \sigma_i$ as the scalar product of the magnetic moment $\frac{1}{2}\gamma\vec{\sigma}$ of the atom (γ, gyromagnetic ratio) with a fictitious magnetic field $\vec{H}_f$ defined by

$$-\tfrac{1}{2}\gamma(H_f)_i = c_i \quad (i = x, y, z) \ . \tag{1.6}$$

Then, the effect of the light beam in the F multiplicity can be described in this case by a center-of-mass light shift c_0 and the action of a fictitious magnetic field $\vec{H}_f$.

b. General case: $F > \frac{1}{2}$. A third group of terms appears in the expansion. $\mathcal{H}_e(F)$, which is a $(2F+1)\times(2F+1)$ matrix, is developed on a complete set of irreducible tensor operators ${}^{FF}T_q^{(k)}$ $(-k \leqslant q \leqslant k$, $k = 0, 1, \ldots, 2F)$:

$$\mathcal{H}_e(F) = \sum_{k,q} c_q^{(k)}(F)\ {}^{FF}T_q^{(k)} \ , \qquad -k \leqslant q \leqslant k, \quad k = 0,\ 1,\ 2, \ldots, 2F \ . \tag{1.7}$$

From Eq. (1.4), it appears that $\mathcal{H}_e(F, \phi)$ is the product of two vector operators $\vec{D}$ with scalar ones (P_F and P_ϕ). The product of two vector operators can give only tensor operators of order $k = 0, 1, 2$. As a consequence of the electric dipole character of the optical transition, $\mathcal{H}_e$ has the following form[20]:

$$\mathcal{H}_e(F) = c_0^{(0)}(F) + \sum_{q=-1}^{1} c_q^{(1)}(F)\ {}^{FF}T_q^{(1)} + \sum_{q=-2}^{2} c_q^{(2)}(F)\ {}^{FF}T_q^{(2)} \ , \tag{1.8}$$

where $c_0^{(0)}(F)$ is the c.m. light shift.

As ${}^{FF}T_0^{(1)} \propto F_z$, ${}^{FF}T_{\pm 1}^{(1)} \propto \mp(1/\sqrt{2})(F_x \pm i F_y)$, the second part of $\mathcal{H}_e(F)$ can be rewritten as a linear combination of F_x, F_y, F_z. As in the $F = \frac{1}{2}$ case, its effect is equivalent to the action of a fictitious magnetic field $\vec{H}_f$. The third part involves the five operators ${}^{FF}T_q^{(2)}$, which are proportional to

$$\begin{aligned} {}^{FF}T_{\pm 2}^{(2)} &\propto \tfrac{1}{2}(F_x \pm i F_y)^2 \ , \\ {}^{FF}T_{\pm 1}^{(2)} &\propto \mp\tfrac{1}{2}[F_z(F_x \pm i F_y) + (F_x \pm i F_y)F_z] \ , \\ {}^{FF}T_0^{(2)} &\propto (1/\sqrt{6})[3F_z^2 - F(F+1)] \ . \end{aligned} \tag{1.9}$$

This part represents the action of a fictitious electric field gradient on the quadrupole moment of the F level. But we will show later that in some cases, it can also be interpreted as describing the second-order Stark effect of a fictitious static electric field on the ground state.

Apart from the c.m. light shift, which we will ignore in the following, $\mathcal{H}_e$ is entirely determined by the eight coefficients $c_q^{(1)}(F)$ and $c_q^{(2)}(F)$.[21] They can be computed explicitly as a function of the atomic and light-beam parameters as shown in Ref. 3. But our purpose is to look at the angular aspect of $\mathcal{H}_e$. Thus, only the *relative* magnitude of the coefficients is needed. We will show that many of the results on this problem can be obtained from very simple arguments. For instance, the symmetries of the light beam often imply that most of the $c_q^{(k)}$ cancel.

B. Explicit Form of $\mathcal{H}_e$ in Some Particular Cases

1. *Consequences of the Light-Beam Symmetries*

Suppose that the light beam (more precisely, its polarization) is invariant under some geometrical transformation $\mathcal{R}$, such as a rotation or a reflection. $\mathcal{H}_e(F)$, which represents the effect of the light beam inside the F multiplicity, must also remain unchanged by $\mathcal{R}$. If $R(F)$ is the corresponding transformation operator in the F subspace, the invariance of $\mathcal{H}_e(F)$ is expressed by

$$R(F)\mathcal{H}_e(F)R^\dagger(F) = \mathcal{H}_e(F) \ , \tag{1.10}$$

which, according to (1.8), is equivalent to

$$\sum_{k,q} c_q^{(k)}(F) R(F)\ {}^{FF}T_q^{(k)}\ R^\dagger(F) = \sum_{k,q} c_q^{(k)}(F)\ {}^{FF}T_q^{(k)} \ . \tag{1.11}$$

$R(F)\ {}^{FF}T_q^{(k)}\ R^\dagger(F)$ is then reexpressed as a linear combination of the ${}^{FF}T_{q'}^{(k')}$. Identifying the coefficients of the two expansions, one obtains several relations between the $c_q^{(k)}$, which may be used to simplify the expression of $\mathcal{H}_e$.

The consequences of the light-beam symmetries may also be investigated directly on the fictitious fields. These fields, which depend only on the polarization of the light $\vec{e}_\lambda$, may be considered as rigidly fixed to $\vec{e}_\lambda$. Therefore, the fictitious fields are invariant under all the geometrical transformations which leave the polarization of the light beam unchanged.

2. *Determination of Fictitious Fields in Some Simple Cases*

a. One-half spin. Circularly polarized beam. As shown in Sec. I A 3 a, the effect of the light beam is entirely described by a fictitious magnetic

field $\vec{H}_f$. The light beam is invariant under a rotation around its direction of propagation $0z$ so that $\vec{H}_f$ must be parallel to $0z$. Furthermore $\vec{H}_f$ is reversed, if the sense of circular polarization is reversed. The argument is the following. The image of a σ^+ polarized light beam in a mirror parallel to its direction of propagation is a σ^- polarized one. The same transformation changes $\vec{H}_f$, which is an axial vector, in $-\vec{H}_f$. A partially circularly polarized light beam is a superposition of two incoherent σ^+ and σ^- polarized beams, with intensities $\mathcal{I}_+$ and $\mathcal{I}_-$. Its effect is described by a fictitious magnetic field parallel to the beam and proportional to $\mathcal{I}_+ - \mathcal{I}_-$. This result holds also for an elliptically polarized light beam. As a special case, it appears that a nonpolarized beam has no effect on a one-half spin (except the c.m. light shift). The same result holds for a linearly polarized beam.

b. $F > \frac{1}{2}$. *Linearly polarized beam.* The beam B_1 is propagating along the x axis and $\vec{e}_\lambda$ is parallel to $0z$. If B_1 is rotated by an angle φ around the z axis, $\vec{e}_\lambda$ is unchanged. Consequently $\mathcal{K}_e(F)$ must be invariant under this rotation. If $R_{0z}(\varphi)$ is the corresponding rotation operator, the effective Hamiltonian $\mathcal{K}'_e(F)$ associated with the rotated beam B'_1 is

$$\mathcal{K}'_e(F) = R_{0z}(\varphi)\mathcal{K}_e(F)R^{\dagger}_{0z}(\varphi)$$

$$= \sum_{k,q} c_q^{(k)}(F)\left[R_{0z}(\varphi)\,{}^{FF}T_q^{(k)}R^{\dagger}_{0z}(\varphi)\right]. \quad (1.12)$$

As in this rotation ${}^{FF}T_q^{(k)}$ is simply multiplied by $e^{-iq\varphi}$, we have

$$\mathcal{K}'_e(F) = \sum_{k,q}\left[c_q^{(k)}(F)\,e^{-iq\varphi}\right]\,{}^{FF}T_q^{(k)}. \quad (1.13)$$

The invariance requirement $\mathcal{K}_e(F) = \mathcal{K}'_e(F)$ implies $c_q^{(k)}(F) = c_q^{(k)}(F)\,e^{-iq\varphi}$ and consequently

$$c_q^{(k)}(F) = 0 \quad \text{for } q \neq 0\,, \quad (1.14)$$

so that

$$\mathcal{K}_e(F) = c_0^{(1)}(F)\,{}^{FF}T_0^{(1)} + c_0^{(2)}\,{}^{FF}T_0^{(2)}\,. \quad (1.15)$$

$\vec{e}_\lambda$, which is the direction of the electric field of the wave, is also invariant under a reflection in the $x0z$ plane. In this transformation, ${}^{FF}T_0^{(1)} \propto F_z$ changes its sign; ${}^{FF}T_0^{(2)} \propto 3F_z^2 - F(F+1)$ remains unchanged. As $\mathcal{K}_e(F)$ must have the same invariance properties as $\vec{e}_\lambda$, it follows that

$$c_0^{(1)}(F) = 0\,. \quad (1.16)$$

Finally, the effective Hamiltonian which describes the effect of a linearly polarized light beam consists only of the tensor part (it is zero in the $F = \frac{1}{2}$ case according to the Wigner-Eckart theorem). Its general expression is

$$\mathcal{K}_e(F) = b\left[3F_z^2 - F(F+1)\right]\,. \quad (1.17)$$

It looks like the Stark Hamiltonian describing the second-order effect on the ground state produced by a fictitious static field $\vec{E}_f$, parallel to the polarization vector.

$\mathcal{K}_e(F)$ removes only partially the Zeeman degeneracy. The energy shift is the same for the m and the $-m$ sublevels:

$$\omega_m = b\left[3m^2 - F(F+1)\right]\,. \quad (1.18)$$

This is a direct consequence of the invariance of the light beam in a plane reflection.

c. $F > \frac{1}{2}$. *Nonpolarized beam.* A nonpolarized beam (intensity $\mathcal{I}$) is a superposition of two incoherent beams of equal intensities $\frac{1}{2}\mathcal{I}$, linearly polarized at right angle to each other. If the beam propagates along the z direction, the corresponding effective Hamiltonian is

$$\mathcal{K}_e(F) = \tfrac{1}{2}b\left[3F_x^2 - F(F+1)\right] + \tfrac{1}{2}b\left[3F_y^2 - F(F+1)\right]\,, \quad (1.19)$$

which can be expressed as

$$\mathcal{K}_e(F) = -\tfrac{1}{2}b\left[3F_g^2 - F(F+1)\right]. \quad (1.20)$$

This result can also be obtained from the invariance properties of the light beam under rotations around the z axis and $x0z$ plane reflection.

d. $F > \frac{1}{2}$. *Circularly polarized beam.* B_1 is parallel to the z axis. The rotational invariance of B_1 around $0z$ gives

$$\mathcal{K}_e(F) = c_0^{(1)}(F)\,{}^{FF}T_0^{(1)} + c_0^{(2)}(F)\,{}^{FF}T_0^{(2)}$$

$$= aF_z + b\left[3F_z^2 - F(F+1)\right]. \quad (1.21)$$

The circularly polarized light beam is not invariant any more under a plane reflection and its effect inside a level $F > \frac{1}{2}$ is described by a fictitious magnetic field $\vec{H}_f$ *and* a fictitious electric field $\vec{E}_f$, parallel to the direction of propagation. The relative magnitudes of a and b can be obtained only by explicit calculations. When the polarization is reversed, it can be shown, as in Sec. 1 B 2 a, that $\vec{H}_f$ is changed to $-\vec{H}_f$, while the fictitious Stark Hamiltonian is not affected.

e. $F > \frac{1}{2}$. *Light beam equivalent to a pure fictitious magnetic field.* In some cases, it is possible to design light beams which are equivalent only to a fictitious pure magnetic field. Even for $F > \frac{1}{2}$, the tensor part is absent. The idea was suggested by Kastler in the case of the odd isotopes of mercury. The magnetic moment in the $6\,{}^1S_0$ ground state is purely nuclear: $F = I$. In the $6\,{}^3P_1$ excited state, the hyperfine structure is so large with respect to Δk that one can consider one of the sublevels, ϕ, only. The lamp producing B_1 is filled with an even isotope, the resonance line of which coincides in zero magnetic field with the ϕ component. The lamp is placed in a magnetic field, parallel to the direction of B_1. The resonance line

is split into a σ^+ and a σ^- component, located on either side of the absorption line ϕ of the vapor. An example is shown on Fig. 2. (A similar situation exists for the $\phi = \frac{5}{2}$ component of ^{201}Hg excited by ^{204}Hg and for the $\phi = \frac{3}{2}$ component of ^{201}Hg excited by ^{198}Hg.) Their two intensities are equal, so that $\Delta E'_{\sigma+}$ and $\Delta E'_{\sigma-}$ are opposite:

$$\mathcal{H}_{e,\sigma^+} = aI_z + b[3I_z^2 - I(I+1)], \tag{1.22}$$

$$\mathcal{H}_{e,\sigma^-} = -\{-aI_z + b[3I_z^2 - I(I+1)]\} . \tag{1.23}$$

In Eq. (1.23), the minus sign outside the brace comes from $\Delta E'_{\sigma-}$, the one in front of the I_z term comes from the change of polarization. Finally,

$$\mathcal{H}_e = \mathcal{H}_{e,\sigma+} + \mathcal{H}_{e,\sigma-} = 2aI_z , \tag{1.24}$$

and the effect of the light beam is entirely described by a fictitious magnetic field.

f. Alkali atoms. Light shifts in the ground state of alkali atoms have been calculated in great details by Happer *et al.*[14] We present here a simple derivation of $\mathcal{H}_e(F)$ valid only if the hyperfine structure of the excited state is negligible compared to the Doppler width. In this case, $\Delta E'(F, \phi)$ is independent of ϕ. The expression (1.1) of $\mathcal{H}_e(F)$ can be transformed in the following way:

$$\mathcal{H}_e(F) = \Delta E'(F)\, P_F (\vec{e}_\lambda^{\,*} \cdot \vec{D})\, (\textstyle\sum_\phi P_\phi)\, (\vec{e}_\lambda \cdot \vec{D})\, P_F . \tag{1.25}$$

We then use the relation

$$\textstyle\sum_\phi P_\phi = 1_I \otimes P_j ,$$

where 1_I is the unit matrix in the nuclear-variable space and P_j is the projector on the electronic wave function of the excited state. Furthermore, $\vec{D}$ acts only on the electronic variables, so that $\mathcal{H}_e(F)$ becomes

$$\mathcal{H}_e(F) = \Delta E'(F)\, P_F (1_I)(\vec{e}_\lambda^{\,*} \cdot \vec{D}\, P_j \vec{e}_\lambda \cdot \vec{D})\, P_F . \tag{1.26}$$

$\vec{e}_\lambda^{\,*} \vec{D} P_j \vec{e}_\lambda \vec{D}$ is a purely electronic operator acting in the ground state ($L = 0$, $S = \frac{1}{2}$). According to the results of Sec. IB2a

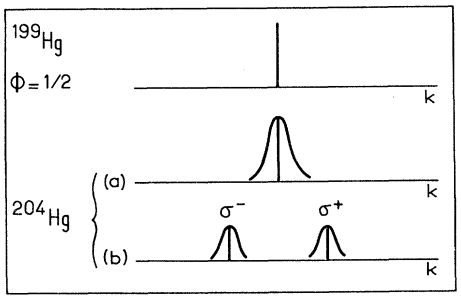

FIG. 2. (a) In zero field, the ^{204}Hg resonance line (2537 Å) coincides with the $\phi = \frac{1}{2}$ component of ^{199}Hg. (b) In an axial magnetic field, the ^{204}Hg lamp emits two components, σ^+ and σ^- polarized, located on either side of the $\phi = \frac{1}{2}$ component of ^{199}Hg.

TABLE I. Effective Hamiltonians and equivalent fictitious fields associated with different types of nonresonant light beams B_1.

B_1 polarization	Effective Hamiltonian	Equivalent fictitious fields
$\vec{u}$	$\mathcal{H} = a F_u + b[F_u^2 - F(F+1)/3]$	$\vec{H}_f$, $\vec{E}_f$
$\vec{e}_\lambda$	$\mathcal{H} = b[F_\lambda^2 - F(F+1)/3]$	$\vec{E}_f$
$\vec{u}$ nonpolarization	$\mathcal{H} = b[F_u^2 - F(F+1)/3]$	$\vec{E}_f$

$$\vec{e}_\lambda^{\,*} \cdot \vec{D}\, P_j \vec{e}_\lambda \cdot \vec{D} = KS_z \tag{1.27}$$

if the light beam propagates along the z axis. $\vec{S}$ is the electronic spin and K a constant depending on J and proportional to the degree of circular polarization of B_1. Finally,

$$\mathcal{H}_e(F) = K\, \Delta E'(F)\, P_F S_z P_F . \tag{1.28}$$

It appears that the tensor part term is absent. Furthermore $\mathcal{H}_e(F)$ has the form of a Zeeman Hamiltonian in the low-field approximation and can be written as $g_F F_z$, where g_F is the Landé factor of the F level (the g_F are of opposite sign for the two hyperfine levels). The effect of the light beam in the two ground-state multiplicities $F = I + \frac{1}{2}$ and $F' = I - \frac{1}{2}$ is described by *two* fictitious magnetic fields, proportional in magnitude and *sign* to $\Delta E'(F = I + \frac{1}{2})$ and $\Delta E'(F' = I - \frac{1}{2})$. For instance, if $k_{F\phi} < \bar{k} < k_{F'\phi}$, the two fictitious fields $\vec{H}_f(F)$ and $\vec{H}_f(F')$ are of opposite signs.

C. Limitations of Concept of Fictitious Field

We want to make clear the limitations of the concept of fictitious field. First, fictitious fields describe the effect of the light beam inside a given level. In other atomic levels, the effect of the same light beam is represented by other fictitious quantities. Second, the choice of the fictitious fields is, to some extent, arbitrary. For instance, the effect of a linearly polarized beam may be described either by a fictitious electric field gradient acting on the atomic quadrupole moment or by a second-order Stark effect produced by a fictitious electric field. One must keep in mind that the effective Hamiltonian is the only quantity with a real physical significance. Nevertheless the fictitious fields are useful for "visualizing" the effect of the light beam, especially its angular aspect. The results of this section are summarized in Table I.

II. EXPERIMENTAL METHODS

Our purpose was first to observe in zero magnetic

field the splitting of the ground state under the action of the nr light wave and secondly to check the form of the effective Hamiltonian and give experimental support to the concepts of fictitious magnetic and electric fields. The splitting in zero magnetic field is measured by resonance or transient methods. The identification of $\mathcal{H}_e$ is more difficult: The eigenstates should be determined. We use in fact another approach. The shape of the Zeeman diagram for various directions of the applied magnetic field is characteristic of the Hamiltonian in zero field. So we compare the experimentally determined Zeeman diagram to the theoretical one, computed from the expected form of $\mathcal{H}_e$. The unknown theoretical parameters introduced in $\mathcal{H}_e$ $(a, b, \ldots)$ are measured directly from the splitting in zero field. The agreement between the two diagrams in nonzero field is a good test for the theoretical expression of $\mathcal{H}_e$. We have carried out this kind of investigation on the ground state of ^{199}Hg ($I = \frac{1}{2}$) and ^{87}Rb (two hyperfine levels, $F = 2$ and $F' = 1$) for circularly polarized nr light beams. The effect of nonpolarized or linearly polarized light beams has been studied in the ground state of ^{201}Hg ($I = \frac{3}{2}$).

In this section we discuss the general characteristics of the experimental setup and procedures.

A. Experimental Setup

1. *Nonresonant Light Beam*

We use conventional light sources, i.e., electrodless discharge lamps. To obtain a nr light, the lamp is either placed in a magnetic field as described in Sec. IB2e, or filled with an isotope different from the one under study in the resonance cell. In order to get $\Delta E'$ maximum, the energy mismatch $\bar{k} - k_{F\Phi}$ is not very large (a few Doppler widths). For instance, we illuminate ^{201}Hg atoms with a ^{200}Hg lamp ($\bar{k} - k_{3/2,\,3/2} = -0.13\ \mathrm{cm}^{-1}$), and ^{199}Hg atoms with a ^{204}Hg lamp in a 2300-G axial magnetic field ($\bar{k} - k_{1/2,\,1/2} = 0.16\ \mathrm{cm}^{-1}$). The shifts on ^{87}Rb are produced by the D_2 line of a ^{85}Rb lamp. As shown in Fig. 3, the ^{85}Rb hyperfine lines lie just

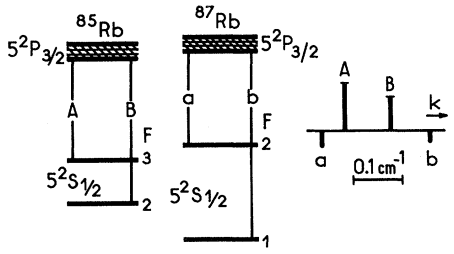

FIG. 3. Hyperfine components of the D_2 line of ^{87}Rb and ^{85}Rb (the hfs in the excited state is negligible compared to the Doppler width).

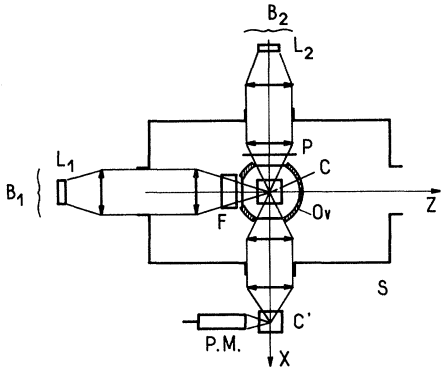

FIG. 4. Setup for experiments on Hg (not to scale). L_1: lamp of the nr light beam B_1. L_2: lamp of the pumping beam B_2. C: Resonance cell. F: filter filled with the same isotope as C. Ov: Oven. P: polarizer. S: magnetic shield. C′: Resonance cell which collects the transmitted B_2 light. P.M.: photomultiplier.

between the two hyperfine components of ^{87}Rb.

As a consequence of the small mismatch $\bar{k} - k_{F\Phi}$, the wings of the nr lines usually contain resonant wavelengths, which produce a broadening of the ground state. This resonant light is suppressed by a filter, filled with the same element as the resonance cell, and placed in front of it. The choice of the filter temperature results from a compromise: at high temperature, the filter absorbs also a fraction of the nr light and diminishes the magnitude of the shift; at a too low temperature, the resonant wavelengths are not absorbed and the ground-state sublevels are broadened. We operate near the temperature which optimizes the ratio of the shift to the width of the sublevels.

To obtain large shifts, a high intensity is required for the nr beam. The size of the discharge lamps is rather large (disks of 3 cm in diameter for mercury lamps, 5 cm for Rb lamps). They are filled with neon or argon buffer gas and excited with a powerful microwave generator (more than 150 W). Polarizers are avoided if possible. For ^{199}Hg the arrangement, described in Sec. IB2e, is used. In the case of ^{201}Hg, fictitious electric fields are produced by nonpolarized beams instead of linearly polarized ones. We use circular polarizers only for the experiments with Rb. The magnitude of the shift is found to depend critically on the operating conditions of the lamps. From one day to another, fluctuations of the order of 10% are observed on the absolute value of the shift. But during a day, it was possible to keep its value constant within a few percent.

2. *Other Parts of Setup*

A diagram of the setup for the experiment on mercury is given in Fig. 4, and that for the experi-

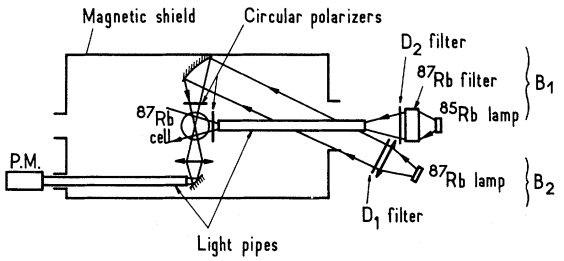

FIG. 5. Setup for experiments on Rb.

ment on rubidium in Fig. 5.

Besides the *nonresonant* shifting beam B_1, a second light beam B_2 is needed. B_2 is *resonant* and its intensity is sufficiently weak so as not to broaden the ground state. B_2 optically pumps the atoms and allows the measurement of their Bohr frequencies in the presence of B_1. The resonances are detected by monitoring the absorption of B_2 by the resonance cell. In the experiment on Hg (Fig. 4), the stray light due to the reflection of the intense B_1 light on the walls of the cell is important and produces an appreciable noise compared to the weak signal detected on B_2. We eliminate it by collecting the transmitted light on a second cell C' which absorbs only the resonant light coming from B_2 (the nr light coming from B_1 goes through). A photomultiplier PM measures the light reemitted by C' at right angles. The Hg or Rb atoms are contained in cells with long relaxation times. The width of the levels is then much smaller than the shift produced by B_1. For mercury isotopes, the fused quartz cells are heated to about 300 °C in order to increase the relaxation time.[22] Paraffin-wall-coated cells are used for ^{87}Rb.[23] The currently obtained results concerning the shifts $\delta'/2\pi$ and the widths $\Gamma'/2\pi$ are summarized in Table II.

Such long relaxation times imply a high sensitivity to the magnetic noise present in the laboratory. We remove it by using magnetic shields. For the mercury experiments, a three-layer Netic and Conetic shield, with a total dynamic shielding factor of 60 is sufficient (the gyromagnetic ratio is a nuclear one). For the experiments on Rb, a large five-layer mumetal shield provides a good protection with a dynamic shielding factor of 10^4–10^5, depending on the direction. Inside the shield, three orthogonal sets of Helmholtz coils can produce fields in all the directions and are used to compensate for the residual field.

B. Experimental Procedures

The only measurable quantities are the differences $\omega_{\alpha\beta} = \omega_\alpha - \omega_\beta$ between the Zeeman energy levels; $\omega_{\alpha\beta}/2\pi$ is a Bohr frequency of the system. When all the $\omega_{\alpha\beta}$ are known, the energy-level pattern can be reconstructed. In this section, we describe different methods for measuring the Bohr frequencies of atoms irradiated by a nr light beam. These measurements are performed in zero or nonzero external magnetic field. Various optical pumping techniques are used: transients, level crossings, different types of resonances, etc. Before describing these methods, let us briefly recall a few results concerning the evolution of the density matrix in an optical-pumping experiment.

1. *Evolution of Density Matrix*

Atoms in the ground state are described by the density matrix σ. The diagonal element $\sigma_{\alpha\alpha} = \langle \alpha | \sigma | \alpha \rangle$ is the population of the α sublevel; $\sigma_{\alpha\beta} = \langle \alpha | \sigma | \beta \rangle$ is the "coherence" between the α and β sublevels. The evolution of σ is due to three processes: effect of the ground-state Hamiltonian (including $\mathcal{H}_e$), relaxation, and optical pumping.

a. Effect of ground-state Hamiltonian. The total Hamiltonian $\mathcal{H}$ is

$$\mathcal{H} = \mathcal{H}_e + \mathcal{H}_m \ .$$

$\mathcal{H}_e$ is the effective Hamiltonian describing the effect of the nr light irradiation, and $\mathcal{H}_m$ is the Zeeman Hamiltonian in an applied external magnetic field. The corresponding rate of variation of σ is

$$\left(\frac{d}{dt}\sigma\right)^{(3)} = -i[\mathcal{H}, \sigma] \ . \tag{2.1}$$

If $|\alpha\rangle$ are the eigenstates of $\mathcal{H}$, with energy ω_α, we have

$$\left(\frac{d}{dt}\sigma_{\alpha\beta}\right)^{(3)} = -i\omega_{\alpha\beta}\sigma_{\alpha\beta} \ , \tag{2.2}$$

$$\omega_{\alpha\beta} = \omega_\alpha - \omega_\beta \ . \tag{2.3}$$

The populations of the $|\alpha\rangle$ states do not change; the coherence $\sigma_{\alpha\beta}$ evolves at the Bohr frequency $\omega_{\alpha\beta}/2\pi$.

b. Relaxation. The atoms are thermalized by various relaxation processes (collision on the walls, essentially). The corresponding evolution of the density matrix is described by a set of linear differential equations, which may be written formally as

TABLE II. Experimental results concerning the splitting δ' in zero field and the width Γ' of the levels.

Atom	State	$\delta'/2\pi$(Hz)	$\Gamma'/2\pi$(Hz)	δ'/Γ'
^{199}Hg	$6^1S_0(I=\frac{1}{2})$	5	0.3	16
^{201}Hg	$6^1S_0(I=\frac{3}{2})$	3	0.2	15
^{87}Rb	$5^2S_{1/2}F=2$	15	3	5
	$F=1$	10	2.3	4.5

$$\frac{d}{dt}^{(2)}\sigma = -\mathfrak{D}(\sigma)\,, \tag{2.4}$$

where $\mathfrak{D}$ is a linear operator in the Liouville space. We assume that $\omega_{\alpha\beta} \ll k_B\Theta$ (k_B Boltzmann constant, Θ temperature), so that the thermal equilibrium is $\sigma = 1$ [$\mathfrak{D}(1) = 0$]. In general, several relaxation time constants appear in the evolution of σ (eigenvalues of $\mathfrak{D}$). In order to simplify the following discussion, we will assume that all these time constants are equal. A more realistic calculation can be performed. The results are qualitatively the same, but the algebra is more complicated.

Thus Eq. (2.4) becomes

$$\frac{d}{dt}^{(2)}\sigma = \Gamma'(1-\sigma)\,, \tag{2.5}$$

where $1/\Gamma'$ is the relaxation time.

c. Optical pumping. It can be shown that the effect of optical pumping by the resonant beam B_2 on σ is also described by an equation of the same type as (2.4):

$$\frac{d}{dt}^{(1)}\sigma = \mathcal{P}(\sigma)\,. \tag{2.6}$$

The time constants involved in $\mathcal{P}(\sigma)$ are of the order of T_p (pumping time associated with B_2). We assume a weak pumping ($1/\Gamma' \ll T_p$). Accordingly, the broadening of the levels due to the pumping beam is small, and the orientation and alignment are weak ($\sigma - 1$ very small). We will therefore approximate (2.6) by

$$\frac{d}{dt}^{(1)}\sigma \simeq \mathcal{P}(1) = \frac{1}{T_p}\,{}^{ex}\sigma\,. \tag{2.7}$$

${}^{ex}\sigma$ describes the state of an initially disoriented atom after an optical pumping cycle. [The replacement of (2.6) by (2.7) implies that this atom will be thermalized before undergoing another pumping cycle.] The total population of the ground state is constant, so that

$$\mathrm{Tr}({}^{ex}\sigma) = 0\,. \tag{2.8}$$

If ${}^{ex}\sigma$ has only diagonal matrix elements, optical pumping is said to be "longitudinal." If ${}^{ex}\sigma$ has also nondiagonal matrix elements, we have "transverse" optical pumping which introduces "coherence" between energy sublevels.

d. Master equation. It can be shown that the total rate of variation of σ is simply[1]

$$\frac{d}{dt}\sigma = \frac{d}{dt}^{(1)}\sigma + \frac{d}{dt}^{(2)}\sigma + \frac{d}{dt}^{(3)}\sigma\,, \tag{2.9}$$

$$= -i\,[\mathcal{H}, \sigma] + \Gamma'(1-\sigma) + (1/T_p)\,{}^{ex}\sigma\,. \tag{2.10}$$

This gives for the evolution of $\sigma_{\alpha\beta}$

$$\frac{d}{dt}\sigma_{\alpha\beta} = -(\Gamma' + i\omega_{\alpha\beta})\sigma_{\alpha\beta} + \frac{1}{T_p}\,{}^{ex}\sigma_{\alpha\beta} + \Gamma'\delta_{\alpha\beta}\,. \tag{2.11}$$

The steady-state solution of this equation is

$$\sigma_{\alpha\beta} = \frac{1}{\Gamma' T_p}\,{}^{ex}\sigma_{\alpha\beta}\,\frac{\Gamma'}{\Gamma' + i\omega_{\alpha\beta}} + \delta_{\alpha\beta}\,. \tag{2.12}$$

Population differences appear between energy sublevels if we choose the polarization of the pumping beam B_2 so that the diagonal elements ${}^{ex}\sigma_{\alpha\alpha}$ are not equal. For transverse optical pumping, the coherences obtained in steady-state conditions depend on the relative magnitude of Γ' and $\omega_{\alpha\beta}$: They disappear if $\Gamma' \ll \omega_{\alpha\beta}$.

2. *Level-Crossing Resonances and Transients*

The energies ω_α of the $|\alpha\rangle$ states depend on the magnetic field H_0. In some cases, level crossings appear in the Zeeman diagram. For a particular value H_c of the magnetic field, the two sublevels $|\alpha\rangle$ and $|\beta\rangle$ have the same energy: $\omega_{\alpha\beta} = 0$. According to (2.12), the steady-state coherence $\sigma_{\alpha\beta}$ undergoes a resonant variation when H_0 is scanned around $H_0 = H_c$. As the amount of light L_A absorbed by the vapor depends linearly on the density matrix elements, this resonant change of $\sigma_{\alpha\beta}$ can be monitored on L_A. The resonances observed in this way are used to determine the position of the crossing points. From the position of the level-crossing resonances, the splitting in zero field is deduced with the help of the theoretical form of the Zeeman diagram. A different way to detect the same effect with a better signal to noise ratio is described in Sec. II B 3. These level-crossing resonances in the ground state are similar to the well-known "Franken resonances"[24] observed on the fluorescent light emitted from two crossing excited sublevels.

The splitting in zero field can also be determined more directly by a transient experiment. The atoms are transversely pumped in zero field, the nr beam B_1 being off. Since all the $\omega_{\alpha\beta}$ are zero, we have in steady-state conditions

$$\sigma(0) = (1/\Gamma' T_p)\,{}^{ex}\sigma + 1\,. \tag{2.13}$$

At time $t = 0$, B_1 is suddenly switched on. The various coherences $\sigma_{\alpha\beta}$ ($\alpha \neq \beta$) reach their new steady-state values (in the presence of B_1)

$$\sigma_{\alpha\beta}(\infty) = \frac{1}{\Gamma' T_p}\,{}^{ex}\sigma_{\alpha\beta}\,\frac{\Gamma'}{\Gamma' + i\omega_{\alpha\beta}} \tag{2.14}$$

in the following way:

$$\sigma_{\alpha\beta}(t) = [\sigma_{\alpha\beta}(0) - \sigma_{\alpha\beta}(\infty)]\,e^{-\Gamma' t}\,e^{-i\omega_{\alpha\beta}t} + \sigma_{\alpha\beta}(\infty)\,. \tag{2.15}$$

Each coherence undergoes a damped oscillation at its Bohr frequency. If $\Gamma' \ll \omega_{\alpha\beta}$, i.e., if B_1 has a sufficient intensity to produce splittings larger than Γ' in zero field, several oscillations at the frequency $\omega_{\alpha\beta}$ can be detected on the absorbed light, with an appreciable amplitude since $\sigma_{\alpha\beta}(\infty) \simeq 0$.

3. *Resonance Methods*

They can be applied to the measurement of the zero-field splitting or to the determination of the Zeeman diagram.

a. Ordinary magnetic resonance. A population difference between the sublevels $|\alpha\rangle$ and $|\beta\rangle$ is produced by the pumping beam B_2. In order to measure the energy difference $\omega_{\alpha\beta}$, an rf field $\vec{H}_1 \cos\omega t$ is applied. The resonance condition $\omega = \omega_{\alpha\beta}$ is detected by a change in the populations of the two sublevels.

b. Modulated transverse pumping. The direction and polarization of the pumping beam B_2 are first chosen in such a way that ${}^{ex}\sigma_{\alpha\beta} \neq 0$ (transverse pumping). The polarization is then modulated by rotating the polarizer (or the quarter-wave plate in the case of a circular polarization) at the angular frequency $\frac{1}{2}\omega$. The pumping rate is modulated at the frequency $\omega/2\pi$ (the initial polarization is restored after half a turn). In Eq. (2.11), ${}^{ex}\sigma_{\alpha\beta}$ must be replaced by

$$ {}^{ex}\sigma_{\alpha\beta} = {}^{ex}\sigma_{\alpha\beta}^{(0)} + {}^{ex}\sigma_{\alpha\beta}^{(1)} e^{i\omega t} + {}^{ex}\sigma_{\alpha\beta}^{(-1)} e^{-i\omega t} \qquad (2.16) $$

and $\sigma_{\alpha\beta}$ undergoes a forced oscillation at the frequency $\omega/2\pi$.[25] The amplitude of $\sigma_{\alpha\beta}$ is large only near resonance ($\omega \approx \omega_{\alpha\beta}$). Neglecting nr terms, one gets for the solution of (2.11)

$$ \sigma_{\alpha\beta} = \frac{1}{\Gamma' T_p} {}^{ex}\sigma_{\alpha\beta}^{(-1)} e^{-i\omega t} \frac{\Gamma'}{\Gamma' + i(\omega_{\alpha\beta} - \omega)} . \qquad (2.17) $$

When ω is swept around $\omega_{\alpha\beta}$, $|\sigma_{\alpha\beta}|$ undergoes a resonant variation centered at $\omega = \omega_{\alpha\beta}$.

The pumping efficiency and $\sigma_{\alpha\beta}$ are both modulated at the frequency $\omega/2\pi$, so that the absorbed light, which depends on the product of these two factors, contains a modulation at the pulsation 2ω, the amplitude of which can be used to monitor the resonance. A phase-sensitive detection of the 2ω modulation gives Lorentz-shaped resonance curves with a half-width equal to the reciprocal Γ' of the relaxation time. The experiment is not difficult to perform in the 0.5–50-Hz frequency range. The rotating polarizer (diameter 5 or 10 cm) lies on an air cushion bearing, and is driven by a frequency-stabilized motor (frequency stability 10^{-2} Hz), or by an air stream.

c. Parametric resonances. Parametric resonances can be used only if the eigenstates $|\alpha\rangle$ are independent of H_0 with energies ω_α varying linearly with H_0:

$$ \omega_\alpha(H_0) = \omega_\alpha(0) + g_\alpha \omega_0 , \qquad (2.18) $$

g_α is a real constant, $\omega_0 = -\gamma H_0$; $\omega_\alpha(0)$ is the energy in zero field. This occurs when $\vec{H}_0$ is parallel to the fictitious fields $\vec{H}_f$ or $\vec{E}_f$. The vapor is transversely pumped by B_2 and the amplitude of $\vec{H}_0$ is modulated at a frequency $\omega/2\pi$, *large* compared to Γ' ($\omega \gg \Gamma'$), by means of an rf field $\vec{H}_1 \cos\omega t$ parallel to $\vec{H}_0$.

$$ \omega_\alpha(H_0 + H_1\cos\omega t) = \omega_\alpha(0) + g_\alpha\omega_0 + g_\alpha\omega_1\cos\omega t = \omega_\alpha(H_0) + g_\alpha\omega_1\cos\omega t , \qquad (2.20) $$

where $\omega_1 = -\gamma H_1$. Consequently, the rate of variation of $\sigma_{\alpha\beta}$ is

$$ \frac{d}{dt}\sigma_{\alpha\beta} = -[\Gamma' + i\omega_{\alpha\beta}(H_0) + i g_{\alpha\beta}\omega_1\cos\omega t]\sigma_{\alpha\beta} + \frac{1}{T_p}{}^{ex}\sigma_{\alpha\beta} , \qquad (2.21) $$

where $g_{\alpha\beta} = g_\alpha - g_\beta$. The coherence is now frequency modulated. The steady-state solution of (2.21) is well known[26–28]:

$$ \sigma_{\alpha\beta} = \frac{1}{T_p}{}^{ex}\sigma_{\alpha\beta} \sum_{n,p} \times \frac{(-)^p J_n(g_{\alpha\beta}\omega_1/\omega) J_{n+p}(g_{\alpha\beta}\omega_1/\omega) e^{ip\omega t}}{\Gamma' + i(\omega_{\alpha\beta} - n\omega)} . \qquad (2.22) $$

$J_q(x)$ is the qth order Bessel function for the value x of the argument. $\sigma_{\alpha\beta}$ contains modulations at the angular frequencies $p\omega$, the amplitudes of which are resonant for

$$ \omega_{\alpha\beta} = n\omega . \qquad (2.23) $$

Phase-sensitive detection gives Lorentz-shaped curves, with a width Γ' independent of the rf field intensity. The $n = 1$ resonance, which occurs for $\omega_{\alpha\beta} = \omega$, provides a measurement of $\omega_{\alpha\beta}$. The resonance $n = 0$ is also interesting. It appears when $\omega_{\alpha\beta} = 0$, i.e., at the crossing point of the two levels $|\alpha\rangle$ and $|\beta\rangle$. "High"-frequency modulation of the static field thus provides modulated level-crossing signals ("high" frequency means $\omega \gg \Gamma'$). We always use them to detect the level crossings with a good signal to noise ratio.

d. Discussion. The resonances described in Sections II B 3 b and II B 3 c ("coherence resonances") have the following advantages: width Γ' and detection on modulated signals (the ordinary magnetic resonance is rf broadened and usually detected on static signals). The modulated transverse pumping resonances are the most versatile ones. Measurements are done at a given value of H_0. This is particularly interesting when the energy levels do not vary linearly with H_0.

III. EXPERIMENTAL EVIDENCES FOR FICTITIOUS FIELDS

A. Fictitious Magnetic Fields

We have studied the effects of circularly polarized nr light beams in the ground state of ^{199}Hg ($I = \frac{1}{2}$) and ^{87}Rb ($F = 2$, $F' = 1$).

1. *Ground State of* ^{199}Hg

In the case of ^{199}Hg (see Fig. 4), the nr shifting beam B_1 is produced by a ^{204}Hg lamp in an axial magnetic field and is propagating along $0z$. As seen in Sec. I B 2, its effect is equivalent to a

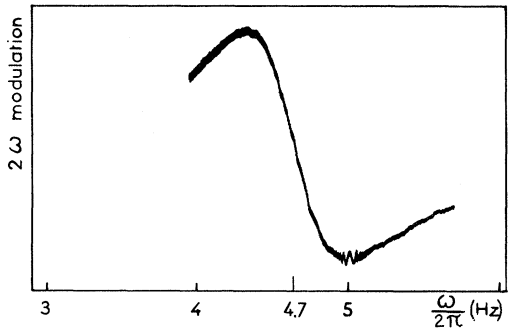

FIG. 6. Resonance observed in zero field by the transverse modulated pumping method. The circular polarization of B_2 is modulated at a frequency $\omega/2\pi$. When ω is swept, a resonance is detected on the 2ω modulation of the transmitted light, centered at $\omega/2\pi = 4.7$ Hz. This gives the splitting due to the nr beam B_1.

fictitious *magnetic* field $\vec{H}_f$, parallel to the z axis. The pumping and detecting beam B_2 is produced by a ^{204}Hg lamp L_2.

a. The removal of the Zeeman degeneracy in zero field is demonstrated by the following two experiments. First, the circular polarization of B_2 is modulated at the frequency $\omega/2\pi$ as described in Sec. II B 3. A resonance is found (Fig. 6) for $\omega/2\pi \simeq 4.7$ Hz which gives the splitting in zero field due to B_1. This resonance frequency can also be interpreted as the Larmor frequency in the fictitious field $\vec{H}_f$.

A second experiment using transients confirms this result. B_1 being off, the ^{199}Hg atoms are oriented in the x direction by B_2, circularly polarized (its polarization is no more modulated). B_1 is then suddenly introduced. The Larmor precession of the spins around $\vec{H}_f$ produces a modulation of the transmitted light at the previously determined frequency (Fig. 7). This clearly shows that spins do precess in fictitious magnetic fields.

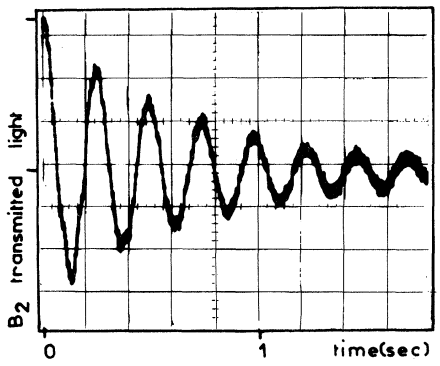

FIG. 7. Larmor precession, in zero magnetic field, of the ^{199}Hg nuclear spins in the fictitious field $\vec{H}_f$ associated with B_1.

b. We have also checked the shape of the Zeeman diagram of the perturbed atoms. A real magnetic field $\vec{H}_0$ is added in the x or z direction. The total field (real plus fictitious) "seen" by the atom is $\vec{H}_f + \vec{H}_0$.

If $\vec{H}_0$ is parallel to $0z$, the eigenstates are always the $|m\rangle_z$ sublevels (eigenstates of $F_z = I_z$) and the corresponding energies are $m(\omega_0 + \omega_f)$ with $\omega_f = -\gamma H_f$. The effect of B_1 is simply to displace the Zeeman diagram by a quantity $-\vec{H}_f$ [Fig. 8, curve (a)]. For different values of H_0, the energy difference between the two sublevels is measured by the parametric resonance method (see Sec. II B 3 c). The energies of the $|+\frac{1}{2}\rangle$ and $|-\frac{1}{2}\rangle$ sublevels, which are simply plus and minus one-half of the energy difference, are in good agreement with the theoretical curve (crosses on Fig. 8).

If $\vec{H}_0$ is perpendicular to $0z$, the intensity of the total field is $(H_f^2 + H_0^2)^{1/2}$ so that the Zeeman diagram is a hyperbola [Fig. 8, curve (b)]. The energy levels are the eigenstates of the component of $\vec{I}$ along the direction of $\vec{H}_f + \vec{H}_0$. They are determined in low fields by the light beam (they coincide with the $|m\rangle_z$ states); in high fields, they are determined by the external magnetic field (they coincide with the $|m\rangle_x$ states). For each value of H_0, the experimental points (circles on Fig. 8) are obtained by the transverse modulated-pumping method (see Sec. II B 3 b).

The very good agreement between the experimentally determined Zeeman diagram and the theoretical one shows that the effect of the light beam is exactly described by a fictitious magnetic field. In particular, the crossing of Fig. 8 [curve (a)] shows that the effect of the light beam can be exactly canceled by a real magnetic field $-\vec{H}_f$. Note also that the magnetic properties of the atom interacting with the light beam are strongly anisotropic as it appears from the various shapes of the Zeeman diagram, depending on the direction of the magnetic field $\vec{H}_0$.

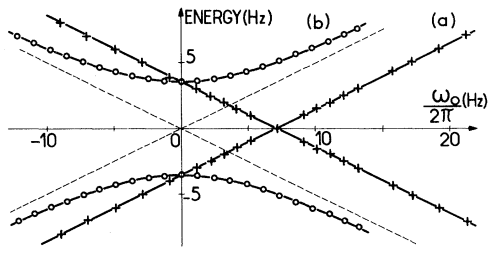

FIG. 8. Zeeman diagram of the ground state of ^{199}Hg atoms perturbed by B_1. (a) Static field $\vec{H}_0$ parallel to B_1; (b) $\vec{H}_0$ perpendicular to B_1 (experimental points, theoretical curves). Dashed lines: normal Zeeman diagram.

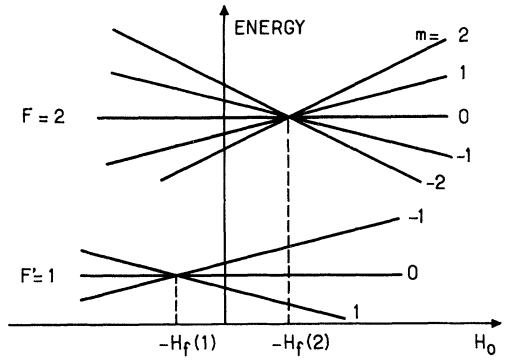

FIG. 9. Zeeman hyperfine diagram of ^{87}Rb atoms perturbed by B_1 ($\vec{H}_0$ parallel to B_1). The two fictitious fields $\vec{H}_f(1)$ and $\vec{H}_f(2)$, describing the effect of B_1 inside the $F'=1$ and $F=2$ hyperfine levels, are of opposite signs.

2. *Ground State of* ^{87}Rb

We have also studied the case of ^{87}Rb because it gives the opportunity to show that the fictitious magnetic fields which describe the effect of the same light beam in different levels may be quite different. We produce light shifts in the ground state of ^{87}Rb using the D_2 line emitted by a ^{85}Rb lamp. The light beam is circularly polarized (Fig. 5). The two ^{85}Rb hyperfine lines lie just between those of ^{87}Rb (Fig. 3). According to Sec. I B 2 f, the fictitious fields $\vec{H}_f(1)$ and $\vec{H}_f(2)$ which describe the effect of the nr beam in the $F'=1$ and $F=2$ hyperfine levels, are of opposite signs. Let us introduce a real magnetic field $\vec{H}_0$, parallel to $\vec{H}_f(1)$ and $\vec{H}_f(2)$. The $F'=1$ and $F=2$ levels "see", respectively, the magnetic field $\vec{H}_0+\vec{H}_f(1)$ and $\vec{H}_0+\vec{H}_f(2)$. The zero-field level crossings are therefore displaced, in opposite directions for the two hyperfine levels (Fig. 9). We detect these level crossings by the method described in Sec. II B 3 c: The resonant beam B_2, circularly polarized, provides a transverse optical pumping; the rf field $\vec{H}_1 \cos\omega t$ modulates $\vec{H}_0$ ($\omega/2\pi = 120$ Hz).

We monitor the 2ω modulation which gives an absorption level crossing signal. In Fig. 10, the curves (a) and (b) are the resonances observed when B_1 is, respectively, off and on. When B_1 is off, the level crossing resonances of the two levels $F'=1$ and $F=2$ coincide in zero field; when B_1 is on, we observe a splitting of the resonance. The $F=2$ resonance undergoes a displacement of 15 Hz, the $F'=1$, a displacement of -10 Hz. The relative intensity of the two resonances is related to the different efficiencies of optical pumping in the two hyperfine levels. The theoretical ratio of the intensities is 5. We detect $\langle S_x \rangle$, which is proportional to the *difference* of the average values of F_x inside the $F=2$ and $F'=1$ multiplicities; this explains the opposite sign of the two resonances.[29] We have verified that the signs of these displacements are changed when the sense of circular polarization of B_1 is reversed [$\vec{H}_f(1)$ and $\vec{H}_f(2)$ are reversed]. We have also checked that the displacements are proportional to the intensity of B_1 (Fig. 11). Finally we have also established that the two reso-

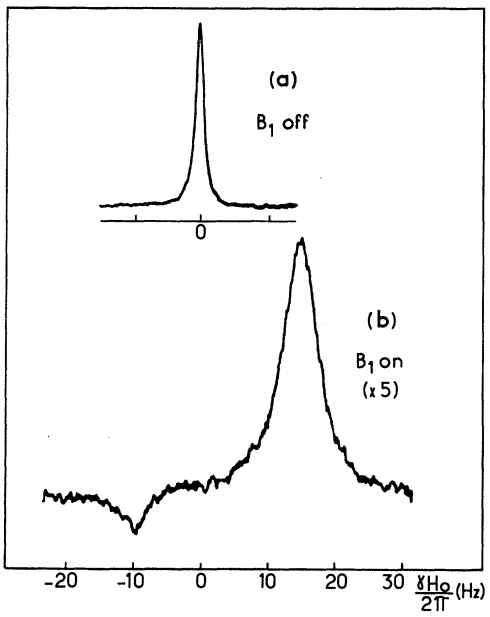

FIG. 10. (a) Zero-field level-crossing signal in the ground state of ^{87}Rb atoms. B_1 is off. (b) B_1 is on. Two resonances corresponding to the two levels crossings of Fig. 9 are now detected. Their relative intensities and their signs agree with the theoretical predictions.

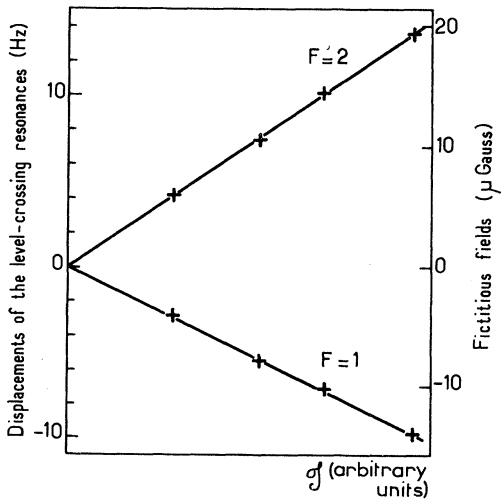

FIG. 11. Variation of the displacement of the level-crossing resonances of Fig. 10(b) with the light intensity g of B_1. The corresponding fictitious fields are given on the right-hand side.

nances of Fig. 10 are, respectively, associated with the two hyperfine levels. We proceed as follows. The magnetic field H_0, always parallel to B_1, is now larger ($\gamma H_0 \approx 120$ Hz). We observe the magnetic resonance line induced by a linearly polarized rf field, perpendicular to $\vec{H}_0$ [Fig. 12(a)]. When B_1 is on, we observe a splitting of the resonance with the same characteristics as before (separation and relative intensities) [Fig. 12(b)]. As the two hyperfine levels have opposite Landé factors, we can identify the two resonances by using a rotating rf field, which induces resonant transitions in only *one* of the two hyperfine levels. This appears clearly on Figs. 12(c) and 12(d). For a σ^+ rf field, only the $F=2$ resonance appears, for a σ^- rf field, only the $F'=1$.

The fact that only one level-crossing resonance appears for each multiplicity is a proof that there is no tensor term in the effective Hamiltonian, as expected since the hfs of the excited state is negligible. A tensor term would produce an additional splitting of each resonance as we shall see in the experiments on ^{201}Hg.

B. Fictitious Electric Fields

We have studied the effect of a nonpolarized nr light beam in the ground state of ^{201}Hg ($I=\frac{3}{2}$, four Zeeman sublevels). In this case, L_1 is a ^{200}Hg lamp (see Fig. 4). The nr light beam B_1 propagating along the z axis, is nonpolarized. The fictitious Stark Hamiltonian

$$\mathcal{H}_e = \tfrac{1}{3} b[3I_z^2 - I(I+1)] \qquad (3.1)$$

describes its effect in the ground state, b being a constant proportional to the light intensity. The pumping beam B_2 propagates along the x axis; it is linearly or circularly polarized. It introduces alignment or orientation in the vapor. In the first case, L_2 is a ^{199}Hg lamp, filtered by a ^{204}Hg filter; C' is filled with ^{201}Hg. In the second case, L_2 is a ^{201}Hg lamp; C' a ^{204}Hg cell.

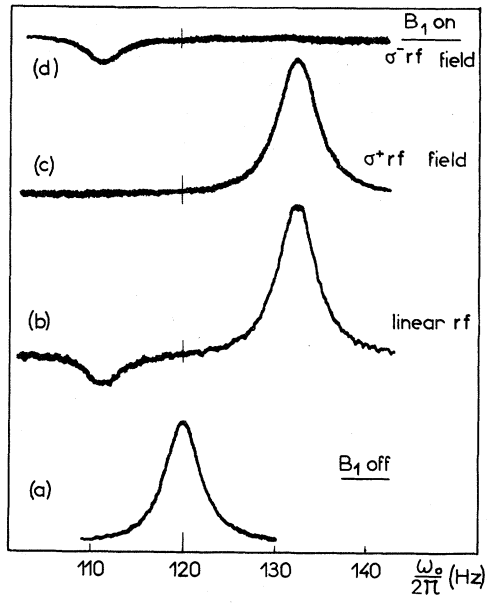

FIG. 12. Magnetic resonance curves in the ground state of ^{87}Rb. (a) B_1 is off. The resonances induced by a linear rf field in the two hyperfine levels coincide. (b) B_1 is on. The two hyperfine levels experience different fictitious fields and the magnetic resonances are separated as in Fig. 10. (c) B_1 is on and the rf field is rotating (σ^+ polarized). The $F=2$ resonance alone is observed. (d) B_1 is on and the rf field σ^- polarized. The $F'=1$ resonance alone is observed.

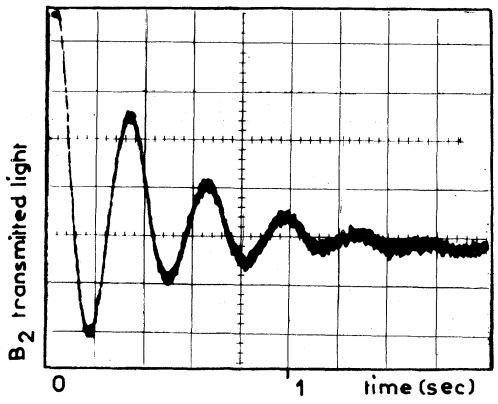

FIG. 13. Oscillation in zero magnetic field of the ^{201}Hg ground-state alignment under the action of the fictitious electric field associated with B_1.

1. *Effect of Light Beam in Zero Field*

The light beam only partially removes the Zeeman degeneracy and splits the ground state into two submultiplicities, viz., the $|+\frac{3}{2}\rangle_z$ and $|-\frac{3}{2}\rangle_z$ sublevels, on the one hand, with energy b and the $|+\frac{1}{2}\rangle_z$ and $|-\frac{1}{2}\rangle_z$ sublevels, on the other hand, with energy $-b$. The zero-field splitting is demonstrated by a transient-type experiment. B_1 being off, B_2 aligns the vapor perpendicularly to $0z$. When B_1 is suddenly introduced, one observes on the transmitted light a modulation at the frequency $2b/2\pi$, which corresponds to the separation between the two multiplicities (Fig. 13). The interpretation of this modulation is completely different from the one given in the previous section. It is not a Larmor precession of a spin orientation in a fictitious magnetic field; it corresponds to an oscillation of the alignment tensor under the action of the fictitious electric field.[30-32]

The zero-field splitting can also be deduced from the position of the crossings observed in the Zeeman diagram.

2. *Zeeman Diagram*

A real magnetic field $\vec{H}_0$ is applied in a direction parallel or perpendicular to the z axis.

a. $\vec{H}_0$ *parallel to fictitious electric field.* The total Hamiltonian is

$$\mathcal{H} = \mathcal{H}_e + \omega_0 I_z , \tag{3.2}$$

where $\omega_0 = -\gamma H_0$. The eigenstates of $\mathcal{H}$ are the $|m\rangle_z$ sublevels, corresponding to the eigenvalues

$$\omega_m = bm^2 + \omega_0 m - bI(I+1)/3 . \tag{3.3}$$

Figure 14 shows the variation of the energy levels with ω_0.

Four level crossings appear in nonzero fields We detect them by the method described in Sec. II B 3 c (parametric resonances $n = 0$, $p = 2$). B_2, propagating along the x axis, is linearly polarized at 45° of $0z$. It introduces coherence between the sublevels $\frac{3}{2}$ and $\pm\frac{1}{2}$ and between $-\frac{3}{2}$ and $\pm\frac{1}{2}$. In Fig. 15(a), B_1 is off. The Zeeman diagram is an ordinary one and only the zero-field level crossing is observed. In Fig. 15(b), B_1 is on and four level-crossing resonances do appear. (There are no resonances in the zero field corresponding to the crossings between $\frac{1}{2}$ and $-\frac{1}{2}$, or $\frac{3}{2}$ and $-\frac{3}{2}$ because the pumping introduces no coherence between these crossing sublevels.) The splitting in zero field, $2b$, can be deduced from the positions of the crossings: The $\Delta m = 1$ crossings occur for $\omega_0 = \pm 2b$, the $\Delta m = 2$, for $\omega_0 = \pm b$.

From the position of the crossings in Fig. 15(b), we get $2b = 3$ Hz. The widths of the $\Delta m = 1$ level-crossing resonances are twice as large as the widths of the $\Delta m = 2$ ones. This is due to the relative slope of the crossing levels which is smaller in the first case (by a factor of 2).

Parametric resonances ($n = 1$, $p = 1$) are used to study the Zeeman diagram. For a linear polarization of B_2, perpendicular to $\vec{H}_0$, one measures the energy differences between sublevels such that $\Delta m = \pm 2$. With a circular polarization, the $\Delta m = \pm 1$ energy differences are also observed. The curves of Fig. 16 represent the theoretical variations with ω_0 of the Zeeman frequencies. The value of $2b$ is taken from the level-crossing experiment described

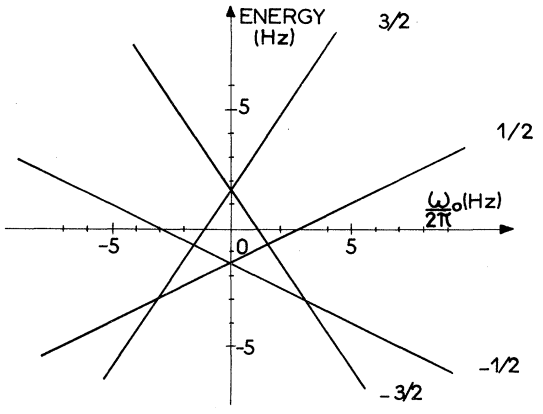

FIG. 14. Theoretical Zeeman diagram of ^{201}Hg atoms in the ground state, perturbed by a fictitious electric field parallel to the magnetic field.

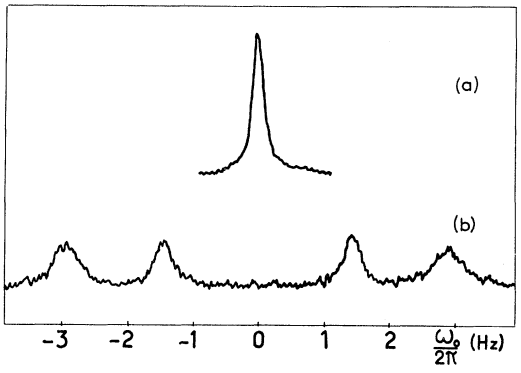

FIG. 15. Observed level-crossing resonances in the ground state of ^{201}Hg atoms. (a) B_1 is off. The single resonance corresponds to the zero-field crossing of the four Zeeman sublevels. (b) B_1 is on. Four level crossings appear in nonzero field according to the Zeeman diagram of Fig. 14.

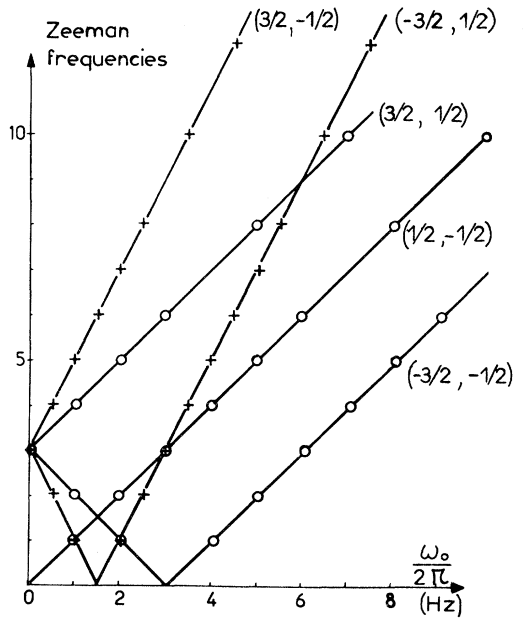

FIG. 16. Variation of the Zeeman transition frequencies with $\omega_0/2\pi$. Theoretical curves are deduced from the diagram of Fig. 14. Crosses and open circles correspond to experimental points, determined, respectively, with a linear and circular polarization of the pumping beam B_2.

above. The points correspond to the experimentally determined frequencies. The agreement is very good. It is impossible, by optical methods, to detect the $\Delta m = 3$ coherence so that it does not appear in the diagram.

In high magnetic field, for a circularly polarized light beam B_2 the magnetic resonance spectrum consists of three lines. The same effect was observed by Cagnac *et al.*[18] in much higher fields.

b. $\vec{H}_0$ *perpendicular to fictitious electric field.* We take $\vec{H}_0$ parallel to $0x$. The total Hamiltonian is

$$\mathcal{H} = \mathcal{H}_e + \omega_0 I_x \ . \tag{3.4}$$

In weak magnetic field ($\omega_0 \ll b$), $\omega_0 I_x$ is a small perturbation compared to $\mathcal{H}_e$. In the $(\frac{3}{2}, -\frac{3}{2})$ submultiplicity, the matrix elements of I_x are zero. The perturbed energy levels are independent of H_0 to first order. In the $(\frac{1}{2}, -\frac{1}{2})$ submultiplicity, $\omega_0 I_x$ removes the degeneracy. The eigenstates are

$$(1/\sqrt{2})(|+\tfrac{1}{2}\rangle_z \pm |-\tfrac{1}{2}\rangle_z) \ , \tag{3.5}$$

corresponding, respectively, to a first-order energy $\pm\omega_0$.

In high field ($\omega_0 \gg b$), the eigenstates of $\mathcal{H}$ are the eigenvectors $|m\rangle_x$ of I_x, with an energy

$$m\omega_0 - \tfrac{1}{6}b\,[3m^2 - I(I+1)] \ . \tag{3.6}$$

In fact, $\mathcal{H}$ can be exactly diagonalized for all values of H_0. The energy diagram [Fig. 17(a)], symmetric with respect to $\omega_0 = 0$, consists of two hyperbolae.

We have measured by the modulated-pumping method (see Sec. II B 3) the frequencies of the six different transitions between the Zeeman sublevels as a function of ω_0. Here again the experimental points [Fig. 17(b)] fit exactly the theoretical curves ($2b$ is adjusted to give the splitting in zero field). In high field, we find the same kind of diagram as in the previous case (H_0 parallel to $0z$). Notice also that in this region, there is no experimental point for the $\alpha - \delta$ transition which becomes a $\Delta m = 3$ one.

IV. RESONANCES INDUCED BY TIME-DEPENDENT FICTITIOUS FIELDS

A. Introduction

The interaction time of the light beam with the atom is the coherence time $1/\Delta k$ of the light wave, which can be also considered as the transit time of a wave packet at a given point. If the polarization $\vec{e}_\lambda$ of the nr beam changes slowly (evolution time longer than $1/\Delta k$), the atom experiences the successive Hamiltonians corresponding to the successive polarizations. The effect of the light beam is described by a time-dependent Hamiltonian which is simply obtained by replacing in the expression of $\mathcal{H}_e$, $\vec{e}_\lambda$ by $\vec{e}_\lambda(t)$. The fictitious fields associated

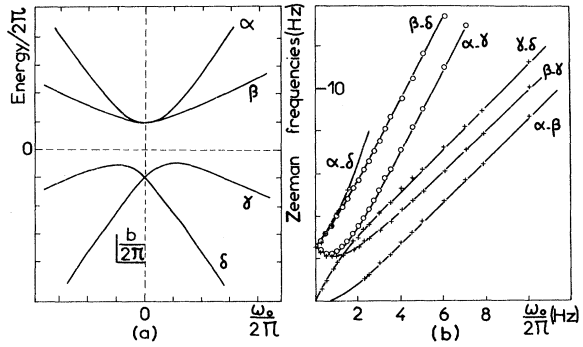

FIG. 17. ^{201}Hg atoms perturbed by a fictitious electric field perpendicular to the magnetic field. (a) Theoretical Zeeman diagram. (b) Variation of the Zeeman transition frequencies with $\omega_0/2\pi$. The theoretical curves are deduced from the diagram of Fig. 17(a). Crosses and open circles correspond to experimental points, determined, respectively, with a linear and circular polarization of B_2.

with the light beam are now time dependent and can induce transitions between the various Zeeman sublevels. The selection rules, the intensity and the rf broadening of the resonances are the same as those with an ordinary rf field. More generally, all kinds of resonances produced by time dependent real magnetic or electric fields can be also observed using fictitious ones[33] with the additional following advantage: Because of the quasiresonant character of the nr beam, the fictitious fields act selectively on a given atomic level of a given atomic species in a mixture. The others species are not perturbed at all.

B. Resonances Induced by Oscillating Fictitious Magnetic Field

We have observed in the ground state of ^{87}Rb various kinds of resonances induced by an oscillating fictitious magnetic field. The quarter-wave plate of the circularly polarized nr beam is rotating at the frequency $\frac{1}{2}\nu$ so that the degree of polarization is proportional to $\cos 2\pi\nu t$.

The effect of the light beam inside the $F = 2$ and $F' = 1$ multiplicities is therefore equivalent to the one of linearly polarized rf fields $\vec{H}_f(2)\cos 2\pi\nu t$ and $\vec{H}_f(1)\cos 2\pi\nu t$, respectively. $H_f(2)$ is, for instance of the order of $16\,\mu$G [$\omega_f = -\gamma H_f(2) = 11$ Hz].

We have observed the magnetic resonance line induced by this fictitious rf field. The static magnetic field is swept perpendicularly to B_1 in the direction of the pumping beam B_2. The value of ν is 120 Hz. The resonances are monitored on the B_2 transmitted light. We observe a superposition of the $F' = 1$ and $F = 2$ resonances. But as seen above (III A 2), their relative intensity is 5 so that we observe mainly the $F = 2$ resonance. Figure 18(a)

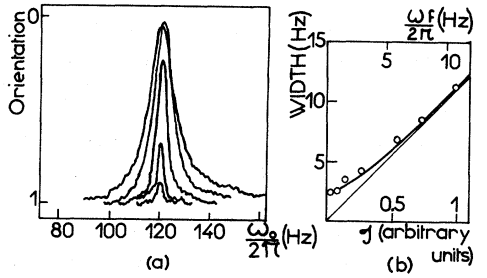

FIG. 18. (a) Magnetic resonances lines on ^{87}Rb induced by an oscillating fictitious field (frequency $\nu = 120$ Hz). The different curves correspond to increasing intensities of the nr light beam B_1 producing the fictitious field. (b) Variation of the width of the resonance with the intensity $\mathcal{I}$ of B_1. The curve is theoretical. The upper scale gives the amplitude (in Hz) of the corresponding fictitious field.

shows the resonance line for different values of the nr light intensity $\mathcal{I}$. The height and the width of the resonance vary as expected with the amplitude of the fictitious rf field $\vec{H}_f(2)$ (which is proportional to $\mathcal{I}$) [Fig. 18(b)]. Let us mention that a similar resonance has already been observed by Happer and Mathur,[9] but the fictitious rf field ($\omega_f/2\pi \approx 7.10^{-2}$ Hz) was much weaker, requiring a more elaborate detection technique. In our experiment, $\omega_f/2\pi \approx 11$ Hz is larger than the relaxation time so that we can easily saturate this transition as it appears on Fig. 18.

Parametric resonances, described in Sec. II B 3, can also be induced by fictitious rf fields. The static field $\vec{H}_0$ is parallel to the rf field (frequency ν) and a transverse pumping is provided by B_2. The modulations of the B_2 transmitted light, at the frequency $p\nu$, are monitored. Resonances appear for $\omega_0/2\pi = n\nu$. Figure 19 shows the parametric resonance spectrum induced by the fictitious rf field

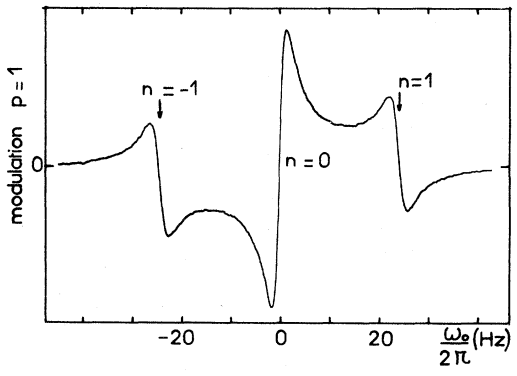

FIG. 19. Parametric resonance spectrum induced on ^{87}Rb by an oscillating fictitious field ($\nu = 24$ Hz). The resonances are detected on the $p = 1$ modulation of the B_2 transmitted light.

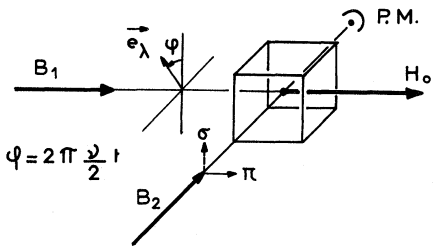

FIG. 20. Resonances induced by a rotating fictitious electric field: diagram of the experiment. The fictitious electric field, parallel to $\vec{e}_\lambda$, is rotating at the frequency $\frac{1}{2}\nu$.

($\nu = 24$ Hz), detected on the $p = 1$ modulation. The $n = 0, \pm 1$ resonances appear clearly. As γH_f is not large enough, the intensities of the others ($|n| > 1$) are much weaker.

The zero-field resonance ($n = 0$), detected on the $p = 1$ modulation, is particularly interesting. Its dispersion shape, its very narrow width (1 μG), and the good signal to noise ratio make this resonance an ideal tool for detecting very small variations of the static field around zero. Variations of 10^{-9} G have been detected by this technique using a real rf field.[34] We have repeated the experiment with a fictitious one. The signal to noise ratio is not as good, but changes of 10^{-8} G can be easily detected. The advantage of fictitious rf fields is that they do not perturb the magnetic shield inside which the experiment is performed, and the sources of the very weak static field to be measured.

C. Resonances Induced by Rotating Fictitious Electric Field

In this experiment, the nr light beam B_1 is linearly polarized. Its effect on the ground state of ^{201}Hg is equivalent to the one of an electric field $\vec{E}_f$ parallel to the polarization vector $\vec{e}_\lambda$. A rotation of the polarizer at frequency $\frac{1}{2}\nu$ gives a rotating fictitious electric field at the same frequency. In the fictitious Stark Hamiltonian, terms modulated at frequency ν appear. We proceed as follows (Fig. 20): ^{201}Hg atoms are irradiated by B_1 and placed in a static field $\vec{H}_0$ perpendicular to $\vec{E}_f$ (i.e., parallel to B_1). They are optically pumped by a light beam B_2, linearly polarized in a direction parallel or perpendicular to $\vec{H}_0$ (π or σ polarization). This looks like an ordinary magnetic resonance experiment, with the only difference being that the rf is replaced by a rotating fictitious electric field. An important consequence is that the perturbation (modulated Stark Hamiltonian) obeys the selection rule $\Delta m = 2$ instead of $\Delta m = 1$. Equalization of the populations is observed when $2\omega_0 = \nu$ ($\omega_0 = -\gamma H_0$). If B_2 is σ polarized, the appearance of a transverse alignment is simultaneously detected by a modulation at the frequency ν of

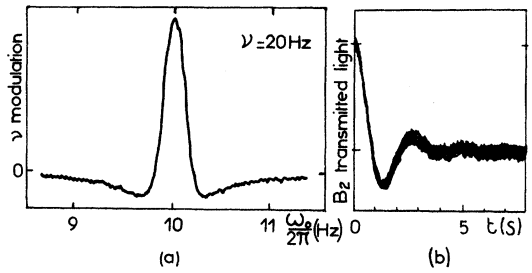

FIG. 21. (a) Shape of the resonance induced by the rotating fictitious electric field. B_2 is σ polarized. The resonance is detected on the ν modulation of the transmitted light. (b) Transient signal when B_1 is suddenly introduced at $t=0$. B_2 is π polarized.

the transmitted light. Figure 21(a) shows the resonance detected on such a modulation ($\nu = 20$ Hz). Its shape can be calculated exactly. This resonance undergoes a broadening when the intensity of the fictitious electric field is increased.[35] The Rabi precession (resonance transient) can also be observed. Figure 21(b) shows the equalization of the population when the rotating fictitious electric field is suddenly introduced.

The same resonances could have been obtained with a rotating real electric field (this has been done, for example, by Geneux[36] in the excited state of Cd). But the intensity of the real electric field required to produce the same effects in the ground state of ^{201}Hg may be evaluated to be of the order of 10^5 V/cm. The fictitious fields are so large because of the quasiresonant character of B_1. This shows clearly the advantage of nr light beams for such an experiment.

ACKNOWLEDGMENTS

We are grateful to Professor A. Kastler and Professor J. Brossel for their constant interest during the course of these experiments and to N. Polonsky-Ostrowsky who has contributed to some parts of this work.

[1]C. Cohen-Tannoudji, Ann. Phys. (Paris) 7, 423 (1962); 7, 469 (1962).

[2]S. Pancharatnam, J. Opt. Soc. Am. 56, 1636 (1966); A. M. Bonch-Bruevich and V. A. Khodovoi, Usp. Fiz. Nauk 93, 71 (1967) [Sov. Phys. Usp. 10, 637 (1967)].

[3]W. Happer and B. S. Mathur, Phys. Rev. 163, 12 (1967).

[4]J. P. Barrat and C. Cohen-Tannoudji, J. Phys. Radium 22, 329 (1961); 22, 443 (1961).

[5]U. Fano, Rev. Mod. Phys. 29, 74 (1957).

[6]A. Omont, J. Phys. (Paris) 26, 26 (1965).

[7]J. C. Lehmann and C. Cohen-Tannoudji, Compt. Rend. 258, 4463 (1964).

[8]P. S. Pershan, J. P. van der Ziel, and L. D. Malmstrom, Phys. Rev. 143, 574 (1966).

[9]W. Happer and B. S. Mathur, Phys. Rev. Letters 18, 727 (1967) and Ref. 3.

[10]E. B. Aleksandrov, A. M. Bonch-Bruevich, N. N. Kostin, and V. A. Khodovoi, Zh. Eksperim. i Teor. Fiz. Pis'ma v Redaktsiyu 3, 85 (1966)[Sov. Phys. JETP Letters 3, 53 (1966)]; Zh. Eksperim. i Teor. Fiz. 56, 144 (1969) [Sov. Phys. JETP 29, 82 (1969)].

[11]D. J. Bradley, A. J. F. Durrant, G. M. Gale, M. Moore, and P. D. Smith, IEEE J. Quantum Electron. QE-4, 707 (1968).

[12]P. Platz, Appl. Phys. Letters 14, 168 (1969); 16, 70 (1970).

[13]M. Arditi and T. R. Carver, Phys. Rev. 124, 800 (1961).

[14]B. S. Mathur, H. Tang, and W. Happer, Phys. Rev. 171, 11 (1968).

[15]P. Davidovits and R. Novick, Proc. IEEE 54, 155 (1966); F. Hartmann, Ann. Phys. 2, 329 (1967).

[16]C. Cohen-Tannoudji, Compt. Rend. 252, 394 (1961).

[17]L. D. Schearer, Phys. Rev. 127, 512 (1962); C. W. White, W. M. Hughes, G. S. Hayne, and H. G. Robinson, *ibid.* 174, 23 (1968).

[18]B. Cagnac, A. Izrael, and M. Nogaret, Compt. Rend. 267, 274 (1968).

[19]In fact, we neglect the matrix elements of the effective Hamiltonian which couples sublevels of different F. Their effects are of the order of $(\Delta E')^2$ (hyperfine splitting)$^{-1}$, and are therefore negligible according to assumption (d).

[20]A similar result exists for resonant light beams. The absorbed light depends only on the population, orientation, and alignment of the ground state.

[21]$\mathcal{K}_e$ is Hermitian so that $(c_q^{(k)})^* = (-)^q c_{-q}^{(k)}$. $\mathcal{K}_e$ depends only on eight real parameters.

[22]B. Cagnac, Ann. Phys. (Paris) 6, 467 (1961); B. Cagnac and G. Lemeigan, Compt. Rend. 264B, 1850 (1967).

[23]M. A. Bouchiat and J. Brossel, Phys. Rev. 147, 41 (1966) and references therein.

[24]P. A. Franken, Phys. Rev. 121, 508 (1961).

[25]The same result is obtained by modulating the pumping light intensity: W. E. Bell and A. L. Bloom, Phys. Rev. Letters 6, 280 (1961).

[26]E. B. Aleksandrov, O. B. Konstantinov, V. I. Perel', and V. A. Khodovoi, Zh. Eksperim. i Teor. Fiz. 45, 503 (1963) [Sov. Phys. JETP 18, 346 (1964)].

[27]C. J. Favre and E. Geneaux, Phys. Letters 8, 190 (1964).

[28]N. Polonsky and C. Cohen-Tannoudji, Compt. Rend. 260, 5231 (1965).

[29]M. A. Bouchiat, thesis, 1964 (unpublished); Publ. Sci. Tech. Min. Air, France, Technical Note No. 146, 1965 (unpublished).

[30]If the initial alignment introduced by B_2 is neither parallel nor perpendicular to the fictitious field $\vec{E}_f$, a spin orientation may appear during the evolution of the system. We have detected this orientation by measuring the circular dichroism of the vapor (Ref. 31). Further theoretical details about this effect may be found in Ref. 32.

[31]C. Cohen-Tannoudji and J. Dupont-Roc, Opt. Commun. 1, 184 (1969).

[32]M. Lombardi, J. Phys. (Paris) 30, 631 (1969).

[33]The physical mechanism of the transitions induced by modulated fictitious fields is however quite different from

an ordinary emission or absorption of a rf photon. As discussed by Happer and Mathur, Ref. (9), they can be considered as optical double transitions related to a stimulated Raman effect.

[34]J. Dupont-Roc, S. Haroche, and C. Cohen-Tannoudji, Phys. Letters 28A, 638 (1969).

[35]J. Dupont-Roc and C. Cohen-Tannoudji, Compt Rend. 267, 1275 (1968).

[36]E. Geneux, Proceedings of the Optical Pumping and Atomic Line Shape Conference, Varsovie, 1968 (unpublished).